Inorg. Chem. **2008**, *47*, 10718−10722

Manganese(III) Corrole-Oxidant Adduct as the Active Intermediate in Catalytic Hydrogen Atom Transfer

Michael J. Zdilla and Mahdi M. Abu-Omar*

Brown Laboratory, Department of Chemistry, Purdue University, 560 Oval Drive, West Lafayette, Indiana 47906

Received June 26, 2008

Hydrogen atom transfer (HAT) reactions from dihydroanthracene to ArINTs (Ar = 2-*tert*-butylsulfonyl)benzene and Ts = *p*-toluenesulfonyl) is catalyzed by Mn(tpfc) (tpfc = 5,10,15-tris(pentafluorophenyl)corrole). Kinetics of HAT was monitored by gas chromatography. Conversion to the major products anthracene, $TsNH_2$, and ArI is too fast to be explained by direct HAT from the terminal imido complex TsN=Mn(tpfc), which forms from the reaction of Mn(tpfc) with ArINTs. Steady-state kinetics, isotope effects, and variation of the initial catalyst form (Mn^{III}(tpfc) vs $TsN=Mn^{V}$(tpfc)) support a mechanism in which the active catalytic species is an adduct of manganese(III) with the oxidant, (ArINTs)Mn^{III}(tpfc). This species was detected by rapid-scan stopped-flow absorption spectroscopy. Kinetic simulations demonstrated the viability of this mechanism in contrast to other proposals.

Introduction

Cytochrome P450 is a versatile heme oxidase essential for drug metabolism and biological detoxification.[1] The traditional mechanism for oxygen atom transfer (OAT) catalyzed by cytochrome P450 involves a high-valent oxo-ferryl porphyrin (Por) cation radical species, $O=Fe^{IV}(Por)^{\bullet+}$, dubbed compound I (Cpd I). While this intermediate has gained wide acceptance as the defining mechanistic feature of this enzyme, recent results on protein mutants, as well as on biomimetic synthetic models,[2−4] have pointed to the possibility of alternative oxidizing intermediates, often referred to as the "multiple oxidant hypothesis." Some of these findings have been recently revisited and attributed to a two-state reactivity model of Cpd I.[5]

Findings from the groups of Collman, Nam, and Que[6] have pointed to a low valent metal-oxidant adduct as the oxidizing species for a number of biomimetic systems (pathway A, Scheme 1) in addition to the traditional OAT pathway from high-valent metal oxo (B). This low valent metal-oxidant intermediate has been referred to as compound 0 because of its analogy with the ferric peroxo species in cytochrome P450. Some of this reactivity has lately been rationalized by a two-state reactivity model,[5] and some reports have demonstrated compound-0-like intermediates to be more

* To whom correspondence should be addressed. E-mail: mabuomar@purdue.edu.

(1) Groves, J. T.; Han, Y. Z. In *Cytochrome P450: Structure Mechanisms and Biochemistry*; Ortiz de Montellano, P. R., Ed.; Plenum: New York, 1995; Chapter *1*, pp 3−48.

(2) (a) Lee, K. A.; Nam, W. *J. Am. Chem. Soc.* **1997**, *119*, 1916. (b) Primus, J.-L.; Boersma, M. G.; Mandon, D.; Boeren, S.; Veeger, C.; Weiss, R.; Rietjens, I. M. C. M. *J. Biol. Inorg. Chem.* **1999**, *4*, 274–283. (c) Lee, Y. J.; Goh, Y. M.; Han, S.-Y.; Kim, C.; Nam, W. *Chem. Lett.* **1998**, 837–838. (d) Kamaraj, K.; Bandyopadhyay, D. *J. Am. Chem. Soc.* **1997**, *119*, 8099–8100. (e) Pratt, J. M.; Ridd, T. I.; King, L. J. *J. Chem. Soc., Chem. Commun.* **1995**, 2297–2298. (f) Machii, K.; Watanabe, Y.; Morishima, I. *J. Am. Chem. Soc.* **1995**, *117*, 6691–6697. (g) Watanabe, Y.; Yamaguchi, K.; Morishima, I.; Takehira, K.; Shimizu, M.; Hayakawa, T.; Orita, H. *Inorg. Chem.* **1991**, *30*, 2581–2582.

(3) (a) Coon, M. J.; Vaz, A. D. N.; McGinnity, D. F.; Peng, H. M. *Drug Metab. Dispos.* **1998**, *26*, 1190–1193. (b) Vaz, A. D. N.; McGinnity, D. F.; Coon, M. J. *Proc. Natl. Acad. Sci. U.S.A.* **1998**, *95*, 3555–3560. (c) Toy, P. H.; Newcomb, M.; Coon, M. J.; Vaz, A. D. N. *J. Am. Chem. Soc.* **1998**, *120*, 9718–9719. (d) Vaz, A. D. N.; Pernecky, S. J.; Raner, G. M.; Coon, M. J. *Proc. Natl. Acad. Sci. U.S.A.* **1996**, *93*, 4644–4648. (e) Toy, P. H.; Dhanabalasingam, B.; Newcomb, M.; Hanna, I. H.; Hollenberg, P. F. *J. Org. Chem.* **1997**, *62*, 9114–9122. (f) Pratt, J. M.; Ridd, T. I.; King, L. J. *J. Chem. Soc., Chem. Commun.* **1995**, 2297–2298.

(4) (a) Nam, W.; Lim, M. H.; Moon, S. K.; Kim, C. *J. Am. Chem. Soc.* **2000**, *122*, 10805. (b) Collman, J. P.; Zeng, L.; Decréau, R. A. *Chem. Commun.* **2003**, 2974. (c) Song, W. J.; Ryu, Y. O.; Song, R.; Nam, W. *J. Biol. Inorg. Chem.* **2005**, *10*, 294.

(5) (a) Hirao, H.; Que, L.; Nam, W.; Shaik, S. *Chem.—Eur. J.* **2008**, *14*, 1740. (b) Shaik, S.; Hirao, H.; Kumar, D. *Acc. Chem. Res.* **2007**, *40*, 532. (c) Seo, M. S.; Kamachi, T.; Kouno, T.; Murata, K.; Park, M. J.; Yoshizawa, K.; Nam, W. *Angew. Chem., Int. Ed.* **2007**, *46*, 2291. (d) Hirao, H.; Kumar, D.; Shaik, S. *J. Am. Chem. Soc.* **2006**, *128*, 8590.

(6) (a) Nam, W.; Choi, S. K.; Lim, M. H.; Rohde, J.-U.; Kim, I.; Kim, J.; Kim, C. *Angew. Chem., Int. Ed.* **2003**, *42*, 109. (b) Collman, J. P.; Chien, A. S.; Eberspacher, T. A.; Brauman, J. I. *J. Am. Chem. Soc.* **2000**, *122*, 11098. (c) Nam, W.; Lim, M. H.; Lee, H. J.; Kim, C. *J. Am. Chem. Soc.* **2000**, *122*, 6641.

10.1021/ic801182q CCC: $40.75
Published on Web 10/15/2008

Scheme 1. Oxidative Intermediates for the Multiple Oxidant Hypothesis

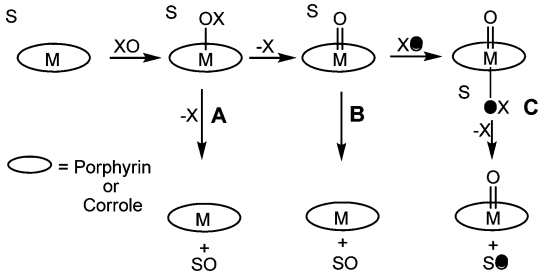

sluggish oxidants than their compound I analogues.[5c] As an additional oxidative species, Goldberg reported on the oxidation of sulfides and phosphines catalyzed by an oxidant adduct of high valent Mn(V)-oxo-corrolazine species (pathway C).[7] We recently reported catalytic aziridination in which styrene is oxidized by transfer of nitrene from an oxidant adduct of high valent manganese imido, that is, the nitrogen analogue of pathway C.[8] Thus, the varied and controversial reactivity of cytochrome-P450 and model compound intermediates makes the exploration of these reaction types of fundamental interest.

In the radical rebound mechanism for oxygen insertion typical of cytochrome P450 chemistry, the first step involves a hydrogen atom transfer (HAT) from the substrate C−H bond to high-valent oxoferryl, resulting in an iron hydroxyl and a caged carbon radical (eq 1).[1]

$$O{=}Fe^{IV}(Por)^{\bullet+} + R{-}H \rightarrow HO{-}Fe^{IV}(Por) + R\bullet \qquad (1)$$

The HAT reaction is also an essential step in the Amoco MC oxygenation process, which is employed in the conversion of 1.5 million tons of *p*-xylene to terephthalic acid per year.[9] For these reasons, HAT reactions are also of fundamental interest.[10] Goldberg has reported on a noteworthy HAT reaction facilitated by a manganese-oxo-corrolazine.[11] The groups of Borovik and Holland have also reported on the formation of iron-amido species as a result of hydrogen atom abstraction from intermediate iron-imido.[12]

We recently reported on a two-mechanism HAT facilitated by high-valent manganese-imido-corrole (TsN=Mn^{V}(tpfc), **2**, tpfc = 5,10,15-tris(pentafluorophenylcorrole)),[13] which is prepared from the Mn(III) corrole (**1**)[8,14] and soluble aryl iodinane.[15] Stoichiometrically, **2** abstracts hydrogen from donors such as phenol and dihydroarenes. The reaction products are Mn^{III}(tpfc), $TsNH_2$, and the corresponding phenoxyl radical or arene.[13] Given the reformation of Mn^{III} upon atom transfer, the reaction is expected to be catalytic in Mn^{III}. We report herein our findings on the catalytic activity of **1** for hydrogen atom transfer from dihydroanthracene to tosyl nitrene. In this report, we uncover a new mechanism for hydrogen atom transfer under catalytic conditions.

Results and Discussion

In addressing the catalytic role of Mn(tpfc) (**1**) in hydrogen atom transfer chemistry, we have explored the transfer of hydrogen atoms from dihydroanthracene (DHA) to ArINTs (2-fold excess) using a catalytic amount of Mn^{III}(tpfc) (0.5 mol% relative to DHA), eq 2.

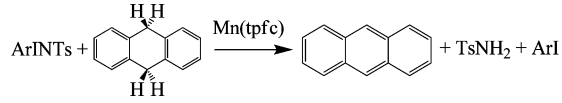

(2)

Reaction under these conditions resulted in 85% conversion of DHA to products, corresponding to a catalytic turnover number (TON) of 170. Of the reacted DHA, 50% is converted to anthracene based on gas chromatography (GC) and NMR analysis. The remaining product is believed to form anthracene polymers and oligomers resulting from radical coupling reactions. While these products were not discernible by GC or NMR analysis, thin-layer chromatography (TLC) analysis (silica, 1:2 ethyl acetate/hexanes) showed at least 8 distinct fluorescing spots as well as a long fluorescent smear consistent with anthracene oligomers and polymers. Similar to the stoichiometric HAT reaction with **2**,[13] but in contrast to an Fe-mediated HAT reaction reported by Borovik,[12a] cross-coupled 9,9′,10,10′-tetrahydrobiantrhacene was not observed among the products (NMR and GC). $TsNH_2$ and ArI are produced in slightly greater than 100% yield based on DHA, which is attributed to decomposition of reactive intermediates (vide infra) and use of 2-fold excess ArINTs. Despite the existence of multiple products, the dominant anthracene yield suggests that C−H bond abstraction is the major pathway for oxidation of dihydroanthracene in the catalytic system.

In an attempt to determine the mechanism of catalytic HAT, we performed kinetic measurements, monitoring the disappearance of DHA by GC, and employed kinetic simulation to examine a number of potential mechanisms for this system. The most obvious mechanism is the abstraction of hydrogen by the terminal imido complex **2**,

(7) Wang, S. H.; Mandimutsira, B. S.; Todd, R.; Ramdhanie, B.; Fox, J. P.; Goldberg, D. P. *J. Am. Chem. Soc.* **2004**, *126*, 18.
(8) Zdilla, M. J.; Abu-Omar, M. M. *J. Am. Chem. Soc.* **2006**, *128*, 16971.
(9) (a) Partenheimer, W. *Catal. Today* **1995**, *23*, 69. (b) Koshino, N.; Saha, B.; Espenson, J. H. *J. Org. Chem.* **2003**, *68*, 9364. (c) Saha, B.; Koshino, N.; Espenson, J. H. *J. Phys. Chem. A* **2004**, *108*, 425–431.
(10) (a) Mayer, J. M. *Acc. Chem. Res.* **1998**, *31*, 441. (b) Markle, T. F.; Mayer, J. M. *Angew. Chem., Int. Ed.* **2008**, *47*, 738. (c) Warren, J. J.; Mayer, J. M. *J. Am. Chem. Soc.* **2008**, *130*, 2774. (d) Mader, E. A.; Davidson, E. R.; Mayer, J. M. *J. Am. Chem. Soc.* **2007**, *129*, 5153. (e) Wang, K.; Mayer, J. M. *J. Org. Chem.* **1997**, *62*, 4248. (f) Gardiner, K. A.; Mayer, J. M. *Science* **1995**, *269*, 1849. (g) Cook, G. K.; Mayer, J. M. *J. Am. Chem. Soc.* **1994**, *116*, 8859. (h) Conry, R. R.; Mayer, J. M. *Inorg. Chem.* **1990**, *29*, 4862. (i) Rhile, I. J.; Markle, T. F.; Nagao, H.; DiPasquale, A. G.; Lam, O. P.; Lockwood, M. A.; Rotter, K.; Mayer, J. M. *J. Am. Chem. Soc.* **2006**, *128*, 6075.
(11) Lansky, D. E.; Goldberg, D. P. *Inorg. Chem.* **2006**, *45*, 5119.
(12) (a) Lucas, R. L.; Powell, D. R.; Borovik, A. S. *J. Am. Chem. Soc.* **2005**, *127*, 11596. (b) Eckert, N. A.; Vaddadi, S.; Stoian, S.; Lachicotte, R. J.; Cundari, T. R.; Holland, P. L. *Angew. Chem., Int. Ed.* **2006**, *45*, 6868.
(13) Zdilla, M. J.; Dexheimer, J. L.; Abu-Omar, M. M. *J. Am. Chem. Soc.* **2007**, *129*, 11505.
(14) Gross, Z.; Galili, N.; Simkhovich, L.; Saltsman, I.; Botoshansky, M.; Bläser, D.; Boese, R.; Goldberg, I. *Org. Lett.* **1999**, *1*, 599.
(15) Macikenas, K.; Skryzpczak, E.; Prostaseiwicz, J. D. *J. Am. Chem. Soc.* **1999**, *121*, 7164.

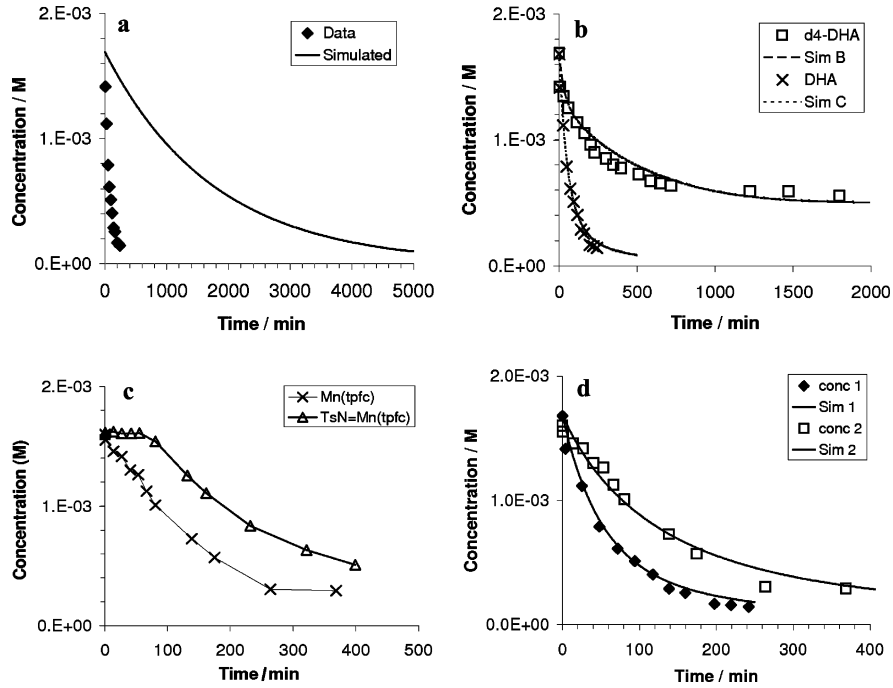

Figure 1. Kinetics plots for disappearance of DHA. (a) $[DHA]_0 = 1.6$ mM, $[\mathbf{1}] = 4.9 \times 10^{-5}$ M. Simulation performed according to the mechanism in eq 1 using known values for K_1, k_2, and k_3. (b) Comparative traces for dihydroanthracene ($R = 0.992$) vs dihydroanthracene-d_4 ($R = 0.967$). $[DHA]_0 = 1.6$ mM, $[\mathbf{1}] = 4.9 \times 10^{-5}$ M. Simulations performed using rate constants in Table 1. (c) Comparative kinetic traces using Mn^{III}(tpfc) (**1**) vs TsN=Mn(tpfc) (**2**) as initial form of manganese catalyst. Conditions: $[Mn(tpfc)] = 2.5 \times 10^{-5}$ M. $[DHA]_0 = 1.6$ mM. Solid lines represent simulations using rate constants in Table 1. (d) HAT kinetics using two different catalyst concentrations of [Mn(tpfc)]. Conc 1 $= 4.9 \times 10^{-5}$ ($R = 0.992$), Conc 2 $= 2.5 \times 10^{-5}$ M ($R = 0.987$). $[DHA]_0 = 1.6$ mM.

which we have previously shown to form from an equilibrium adduct of **1** and ArINTs:[8]

$$\mathrm{Mn^{III}(tpfc) + ArINTs} \underset{}{\overset{K_1}{\rightleftharpoons}} \mathrm{(ArINTs)Mn^{III}(tpfc)}$$
$$\mathrm{(ArINTs)Mn^{III}(tpfc)} \xrightarrow{k_2} \mathrm{TsN{=}Mn^{V}(tpfc) + ArI} \qquad (3)$$
$$\mathrm{TsN{=}Mn^{V}(tpfc) + DHA} \xrightarrow{k_3} \text{[anthracene]} + \mathrm{TsNH_2 + Mn^{III}(tpfc)}$$

The constants K_1-k_3 have been reported previously.[8,13] Use of these values in a kinetic simulation demonstrates that this mechanism is not viable (Figure 1a). In short, catalytic hydrogen abstraction from DHA is happening approximately 20 times faster than the measured stoichiometric HAT reactions previously reported.[13] This high rate of reactivity suggests that another mechanism is at work.

Previously, we have reported on catalytic aziridination using the same Mn(tpfc) catalyst and ArINTs oxidant, which did not proceed by direct transfer of nitrene from terminal imido **2** but from an adduct of **2** with ArINTs (**3**), eq 4.

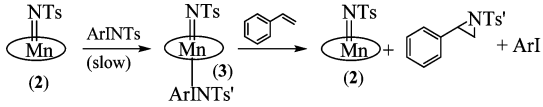

(4)

The formation of **3** is rate-limiting in the azirdination reaction based on zero-order dependence on styrene concentration.[8] In contrast, it is apparent from the traces in Figure 1 that the disappearance of DHA is not zero-order but rather approximates a first-order exponential decay. Additionally, Figure 2b demonstrates the presence of a significant kinetic isotope effect (as well as a 25% drop in DHA conversion) when dihydroanthracene-d_4 is used. No kinetic isotope effect would be expected if formation of **3** was rate-limiting. These observations suggest either that formation of **3** is not rate-limiting or that **3** is not the active species for HAT under catalytic conditions.

Table 1. Rate Constants for Catalytic Hydrogen Atom Transfer of DHA and ArINTs Catalyzed by Mn(tpfc) (**1**)

	DHA Independent	DHA	DHA-d_4
K_1[a]	$10{,}000 \pm 2000$		
k_2[a]	0.26 ± 0.07		
k_3[a]		0.17 ± 0.01	0.049 ± 0.005
k_4[b]		8.3×10^3	1.5×10^3
k_d[b]	3.0		

[a] Rate constant obtained previously.[8,13] Units: K_1, L mol^{-1}; k_2, s^{-1}; k_3, M^{-1} s^{-1}. [b] Rate constants obtained by kinetic simulations. Units: k_4, M^{-1} s^{-1}; k_d, s^{-1}.

To test whether or not a high-valent terminal imido species such as **3** is responsible for catalytic HAT, we have run kinetics experiments with the manganese catalyst in different starting states (**1** versus **2**). If **3** (or any other high-valent form of Mn(tpfc)) is responsible for HAT, a catalyst starting in the form of the high-valent **2** would be expected to perform catalytic HAT at least as fast as or faster than an identical reaction in which trivalent Mn^{III}(tpfc) (**1**) was used as the starting catalyst. Kinetic analysis demonstrates an induction period when **2** is used as the initial form of catalyst (Figure 1c), which dismisses high-valent manganese species as the active catalyst and supports the hypothesis that a Mn^{III} form is responsible.[16] This observation is in contrast to catalytic aziridination, which exhibits identical zero-order kinetic

(16) $TsN{=}Mn^{V}$(tpfc) can return to active Mn^{III} form by stoichiometric HAT from DHA (k_3).

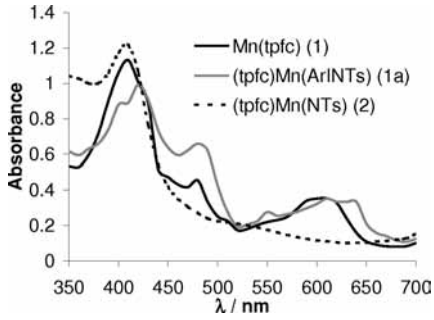

Figure 2. Rapid absorption scans of the reaction of **1** (2.5×10^{-5} M) with 20 equiv of ArINTs to form **1a** after 5 ms. The spectrum of **1a** is obtained by global fitting analysis (Supporting Information). The spectrum subsequently changes to the spectrum of **2** over the course of 15 s.

Scheme 2. Mechanism of Mn(tpfc) Catalyzed Hydrogen Atom Transfer

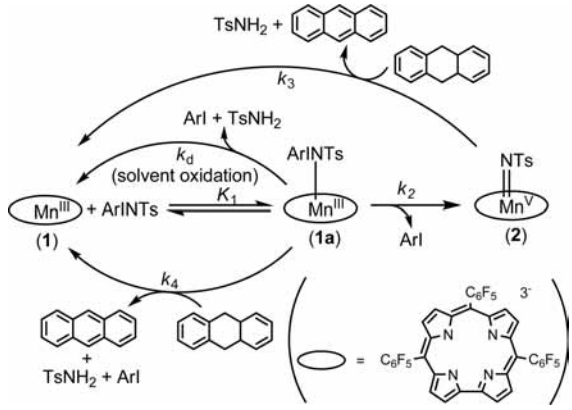

traces regardless of the initial form of catalyst (see Supporting Information).

As we have ruled out direct HAT to the terminal imido **2** as well as to adduct **3**, we propose that an adduct between Mn^{III}(tpfc) and ArINTs (**1a**) is responsible for catalytic HAT with DHA (eq 5).

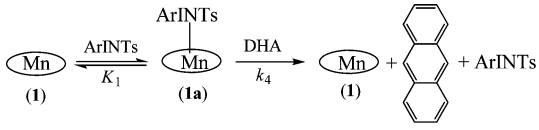

(5)

When the catalyst is allowed to convert completely to the inactive complex **2** (Figure 1c), the reformation of active Mn(III) by stoichiometric HAT (k_3) becomes rate-limiting (Scheme 2). Once in the form of the adduct **1a**, the catalyst competes between unimolecular formation of **2** (k_2) and HAT from DHA by k_4 (Scheme 2).

While the intermediate **1a** has been previously implicated in the mechanism of formation of terminal imido species **2**,[8] it has not been directly observed. We examined the reaction of **1** with 20 equiv of ArINTs using a stopped-flow analyzer in kinetic scan mode in an effort to detect this short-lived species. When **1** and ArINTs are mixed, a minor spectral change is observed over the course of (or faster than) the mixing period of the stopped-flow analyzer (ca. 2 ms). The soret and Q bands of **1** (410, and 600 nm) exhibit a red shift upon reaction, while the weak band of **1** at 480 nm shows an increase in absorbance. The overall band structure is very similar to that of **1** and is thus consistent with manganese(III) corrole in a slightly modified coordination environment. The spectrum is consequently assigned to **1a** (Figure 2). This species transforms unimolecularly to form **2** over the course of about 15 s.[8]

Given the previously reported equilibrium constant for formation of **1a** of 10 000,[8] it should be noted that under our conditions, formation of **1a** is expected to proceed to only 80% completion. The complete spectrum of **1a** (Figure 2) is obtained via global mathematical analysis, assuming the spectrum observed in situ to represent an 80:20 mixture of **1a** and **1**, respectively. The details of this analysis are provided in the Supporting Information.

While **1a** is observable under conditions of excess ArINTs, attempts to generate **1a** in situ and react with DHA using sequential mixing stopped-flow were not possible. Formation of **1a** using equimolar amounts of **1** and ArINTs is problematic because of slowed formation of **1a** (reaction is first order in ArINTs at low concentrations of ArINTs), as well as lower conversion to **1a** (LeChatelier's principle). Additionally, the decomposition of the short-lived **1a** complicates the reaction in the absence of excess ArINTs (k_d, vide infra).

Since direct reaction of **1a** with DHA has not been observed, the possibility of other reactive intermediates must be acknowledged. For instance, a short-lived manganese imido species of alternate spin state in route to formation of **2** could be responsible for reactivity. Such two-state reactivity of high-valent iron oxo compounds have been implicated in cytochrome P450 and model chemistries.[5] As such a species has not been observed in our system, we propose adduct **1a** as the catalytic species at present, though the possibility of other intermediate species cannot be rigorously ruled out.

While the qualitative kinetic behavior seen in Figure 1c is well-supported by the proposed mechanism, the isotopic conversion effect (Figure 1b) is not explained without invocation of a decomposition pathway responsible for directly or indirectly removing ArINTs oxidant from the system. We have shown previously that manganese terminal imido complex **2** decomposes back to Mn(III).[13] This decomposition is attributed to HAT from solvent because of the observation that decomposition occurs more quickly in solvents containing a thermodynamically accessible hydrogen atom such as toluene.[8] Even so, the decomposition of **2** is far too slow in benzene (ca. 1×10^{-4} s^{-1}) to explain the incomplete conversion of d_4-DHA.

Given that **1a** is far more reactive toward DHA than **2**, it is reasonable to invoke that **1a** is also more reactive toward solvent-dependent decomposition. The inclusion of a simple first-order decomposition pathway for **1a** (k_d in Scheme 2) provides kinetic simulations that satisfy (fit) all the data in hand. Rate constants obtained from simulations are presented in Table 1. These rate constants provide accurate fitting of data regardless of starting reagent concentrations (see Figure 1d). It should be noted that k_4 and k_d are determined by simultaneous fitting of the rate data in hand and were not established by independent measurement as was done for K_1-k_3. Hence, rather than provide high-certainty rate con-

stants, the simulation of these rate constants (k_4 and k_d) demonstrates the viability of Scheme 2 where other proposed mechanisms fail.

Conclusion

In summary, we have demonstrated a catalytic HAT reaction for a manganese-corrole system that does not occur via a high-valent imido complex, nor by an oxidant adduct of high-valent imido, which was found previously to be responsible for catalytic aziridination. Instead, an adduct of the oxidant ArINTs with Mn^{III}(tpfc) is proposed to be the active HAT catalyst. This mechanism is supported by (1) variation of initial catalyst speciation, which implicates a mechanism where the low valent complex **1** and not the high-valent Mn imido **2** is responsible for catalysis; and (2) kinetic simulations using known and fitted rate constants, which provided accurate prediction of kinetic behavior regardless of reagent concentrations. It is remarkable to note that among catalytic HAT, catalytic aziridination,[8] and stoichiometric HAT by two distinguishable mechanisms,[13] this versatile Mn(tpfc)/ArINTs catalytic oxidation system exhibits four mechanistically distinct reactions for biologically inspired group transfer reactions.

Experimental Section

General Procedures. All operations were carried out under rigorously dry conditions as water has been previously shown to result in hydrolysis of **2** to form the high-valent iron-oxo species. Benzene solvent was distilled from sodium benzophenone ketyl, degassed, and stored in a dry box over activated molecular sieves for 24 h before use. 9,10-Dihydroanthracene, anthracene, *p*-tolylsulfonamide, and benzophenone were used as received from Aldrich and Acros. Similar results were obtained when dihydroanthracene was recrystallized from toluene/hexane. Mn(tpfc),[8,14] dihydroanthracene-d_4,[13] ArINTs, and ArI[15] were prepared by their respective literature protocols. GC was performed with an Agilent Technologies 6890N Network GC System with a J&W Scientific DB-5 capillary column. Oven temperature was ramped from 70 to 150 at 25 °C/min, then from 150 to 230 at 15 °C/min in constant flow mode at 2.5 mL/min. Peaks in the GC trace were identified and quantified by comparison to calibration curves prepared with the known compounds. NMR spectra were obtained on Inova/Varian 300 MHz spectrometers. Absorption spectroscopy was performed using a Shimadzu UV-2501PC scanning spectrophotometer. Kinetic simulations were performed using the program KINSIM.[17] The mechanism described in Scheme 2 was input into the software. Values of K_1, k_2, and k_3 were fixed at the previously reported literature values. Values of k_4 and k_d were floated to obtain the best fit to the data. Formation of **1a** was observed using an Applied Photophysics SX.18MV stopped-flow analyzer in kinetic scan mode.

Catalytic HAT. For kinetic runs, benzophenone (1−2 mM) was used as an internal standard for GC quantification. Plots of benzophenone signal intensity versus time confirms it is not reactive in this system. For a typical kinetic experiment, ArINTs (24 mg, 49 μmol) was added to a solution of DHA (4.5 mg, 25 μmol), in 2.0 mL of benzene. A 0.5 mL quantity of a 0.25 mM or a 0.12 mM solution of Mn(tpfc) is added last to initiate reaction. In reactions where TsN=Mn(tpfc) (**2**) was the desired starting form of catalyst, the Mn(tpfc) was added to ArINTs and stirred for 10 min to form **2** in situ before the addition of DHA. The reactions were stirred in the glovebox. Approximately every 30 min, a 1 μL aliquot was taken by syringe and analyzed by GC. After the completion of the reaction, the benzene solvent was removed in vacuo, and the residue redissolved in $CHCl_3$, and analyzed by GC for determination of product yields. Yields were determined in this way because of the insolubility of product $TsNH_2$ in benzene.

Detection of 1a by Stopped-Flow. Solutions of **1** (4.88×10^{-5} M) and ArINTs (1.0×10^{-3} M) were prepared in benzene. The latter was heated at 60 °C to encourage dissolution. These were loaded into the drive syringes of the stopped-flow mixer and analyzed in kinetic scan mode over the course of 10 ms. Individual shots monitored over 50 s confirmed previously reported[8] conversion to **2** over longer periods of time.

Acknowledgment. This work was supported by a grant from the U.S. National Science Foundation (CHE-0749572).

Supporting Information Available: Supporting Information for this article includes data on the catalytic aziridination of styrene using Mn^{III}(tpfc) vs (TsN)Mn^{V}(tpfc) as initial catalyst forms, and details on the obtainment of the spectrum of **1a**. This material is available free of charge via the Internet at http://pubs.acs.org.

IC801182Q

(17) Barshop, B. A.; Wrenn, R. F.; Frieden, C. *Anal. Biochem.* **1983**, *130*, 134.